ISSN 1070-4272, Russian Journal of Applied Chemistry, 2009, Vol. 82, No. 5, pp. 757−762. © Pleiades Publishing, Ltd., 2009.
Original Russian Text © L.N. Chukhlomina, Yu.M. Maksimov, 2009, published in Zhurnal Prikladnoi Khimii, 2009, Vol. 82, No. 5, pp. 705−710.

INORGANIC SYNTHESIS AND INDUSTRIAL INORGANIC CHEMISTRY

Relationships in Synthesis of Chromium Nitride by Combustion of Ferrochrome in Nitrogen

L. N. Chukhlomina[a] and Yu. M. Maksimov[b]

[a]*Department of Structural Macrokinetics, Tomsk Scientific Center, Siberian Division, Russian Academy of Sciences, Tomsk, Russia*
[b]*Tomsk Polytechnic University, Tomsk, Russia*

Received July 15, 2008

Abstract—Nitridation of commercial ferrochrome in the self-propagating high-temperature synthesis mode was studied. The influence of the key parameters of the process (nitrogen pressure, sample diameter, particle size distribution of the initial powder) on synthesis and phase composition of the combustion products was elucidated. The microstructural features of nitrided ferrochrome and chromium nitride were examined by electron microscopy. Acid enrichment of the synthesis products in a hydrochloric acid solution was studied in relation to the composition of nitrided ferrochrome. Chromium nitride with the residual iron content of 0.3 wt% was obtained, and its thermal stability and corrosion resistance were examined.

DOI: 10.1134/S1070427209050012

Chromium nitride is superior to other metal-like nitrides in corrosion resistance, is characterized by high reflection coefficient, and exhibits enhanced wear resistance. Chromium nitride serves as alloying addition in smelting of high-chromium stainless steels [1]. Sintered chromium nitride is of interest for manufacture of fuel rods and deposition of oxidation-resistant coatings. However, its extensive application is limited by the lack of efficient commercial production technologies. At the present time, chromium nitride is prepared by furnace (Tula) and plasmochemical procedures (Riga), both of which are highly energy intensive and utilize expensive equipment.

An attractive method for preparing chromium mononitride can be found in self-propagating high-temperature synthesis (SHS) distinguished by the use of the heat of the chemical reaction between the components and an autowave mode of the reaction propagation. Braverman et al. [2] showed that combustion of a chromium powder in gaseous nitrogen is suitable for preparing chromium nitride, the maximal degree of chromium nitridation being 0.94. Also, it was demonstrated [3] that combustion of ferrochrome in nitrogen yields chromium nitrides (Cr_2N + CrN), but this requires preheating of the initial alloy to 300°C.

Published data suggest that, in low-energy systems, SHS does not require additional preheating. This procedure implies preliminary mechanical activation of the reactants, which provides for an energy store enabling SHS [4, 5]. Rabinovich et al. [6] carried out furnace nitridation of ferrochrome and found that it is expedient to crush the initial alloy, and the degree of crushing should increase with decrease in the nitridation temperature.

Taking into account the above-said, we studied here synthesis of chromium mononitride by nitridation of ferrochrome in the SHS mode with a view to developing a new method for preparing technical-grade CrN and Cr. Using commercial ferrochrome as the raw material it will be possible to prepare inexpensive high-quality material.

EXPERIMENTAL

Our study was concerned with commercial metallothermic ferrochrome containing, wt%: chromium 78.6; silicon 0.2; aluminum 0.09; carbon 0.04; phosphorus and sulfur 0.008; iron (balance). Ferrochrome was crushed in an MPV high-energy planetary mill under water cooling at the powder:balls ratio of 1:8. To prevent oxidation of ferrochrome, mechanical activation was carried out in benzine. The time of crushing was varied from 5 to

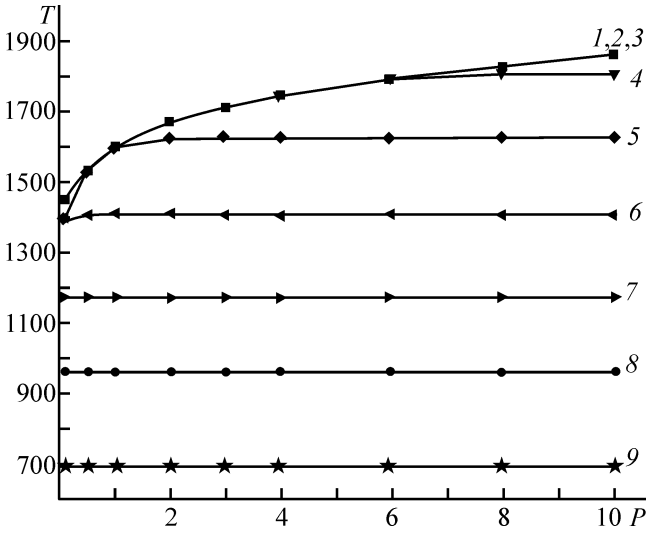

Fig. 1. Calculated dependence of the adiabatic combustion temperature *T*, K, on the nitrogen pressure *P*, MPa, for Fe–Cr alloys containing different amounts of chromium. Chromium content, wt%: (*1*) 90; (*2*) 80; (*3*) 70; (*4*) 60; (*5*) 50; (*6*) 40; (*7*) 30; (*8*) 20; and (*9*) 10.

30 min, depending on the initial ferrochrome particle size. The resulting powder was characterized by the particle size under 80 μm, the dominating fraction being that with the particle size under15 μm. The specific surface area of the powder was estimated by the BET method at 1.1 $m^2 g^{-1}$.

The crushed initial alloy was dried in vacuum desiccator and charged into cylindrical metal grid tubes, 25–60 mm in diameter. The self-propagating high-temperature synthesis was carried out in a constant-pressure setup in a 99.9% pure nitrogen atmosphere. The nitrogen pressure was varied from 0.5 to 10 MPa. The samples were ignited with a powdered igniting composition (a chromium–aluminum alloy) by supplying voltage to a tungsten filament. After passing of the combustion front, the sample was maintained in a nitrogen atmosphere till cooling was complete, whereupon the pressure was relieved, and the SHS product was taken out of the setup and examined.

The X-ray phase analysis was carried out on a DRON-2 diffractometer with Co radiation. The chemical composition of the quenched combustion products was examined by X-ray spectral micro analysis on a CAMEBAX-MICROBEAM setup. The morphology of the initial and synthesized powders was examined using a JEM-100CXII electron microscope with an ASID-4D (JEOL, Japan) raster accessory. The thermal stability and corrosion resistance were examined on an SDT Q 600 (TA Instruments, USA) DTA–TG–DTG analyzer in a helium atmosphere or in air, respectively. Acid enrichment of the SHS products was carried out in a setup equipped with a thermostat and a stirrer. A weighed portion of nitrided ferrochrome was charged into a reaction flask containing the acid, and the flask was placed into a thermostat keeping the preset temperature. This instant was taken as the onset of acid enrichment. The weighed portion was maintained for a certain period in the acid at a constant temperature under vigorous stirring, whereupon the iron and chromium content in the solution was determined .To this end, the nondissolved residue was filtered off, and the filtrate was subjected to chemical analysis. The residue on the filter was washed, dried, and also subjected to chemical and X-ray phase analyses.

The iron content was determined by reduction with aluminum to iron(II), followed by titration with dichromate, as well as by photocolorimetry with sulfosalicylic acid. The total nitrogen content in the combustion products was estimated from the mass increment; more precise measurements were carried out on a LECO TN-114 instrument utilizing hot extraction based on reduction smelting of the analyzed samples in a chemically pure inert gas atmosphere.

To assess whether combustion is possible, we carried out thermodynamic calculation of the adiabatic temperature by the Astra-4 program [7]. It is believed that SHS can be implemented at adiabatic temperatures of the combustion wave 0422_{ad} above 1500°C. Out calculation showed (Fig. 1) that combustion of ferrochrome in nitrogen is possible within fairly narrow ranges of chromium concentration in the alloy and nitrogen pressure (over 60% and 6 MPa, respectively).

In the first stage of our experiments, the SHS–nitridation of ferrochrome was carried out in a constant-pressure setup at a nitrogen pressure over 6 MPa with preheating (without mechanical activation). Preheating utilized convective streams of heated nitrogen, generated by combustion of the igniting composition (a chromium–aluminum alloy). However, ferrochrome combustion was unstable, the combustion front frequently stopped before a half of the height of the sample was reached. The burned part of the sample was characterized by a low conversion and contained, according to the X-ray phase analysis data, primarily chromium nitride Cr_2N, rather than chromium mononitride CrN. We failed to provide stable combustion of ferrochrome in the self-propagation mode over the pressure range examined (up to 10 MPa) in a constant-pressure setup (limited diameter of the sample).

Below, we will discuss the results obtained for ferrochrome powder preliminary crushed in a planetary mill.

Under conditions of filtration supply of nitrogen to the reaction zone, the principal parameter deciding the nitrogen content in the combustion products is the reacting gas pressure. Figure 2 shows how the combustion velocity and the degree of ferrochrome nitriding vary with the nitrogen pressure.

It is seen that the nitrogen content in the combustion products tends to increase with increasing pressure. The combustion velocity also increases with increasing nitrogen pressure because of an increase in the rate of the nitrogen supply to the combustion front. Stable combustion of activated ferrochrome powder can be achieved even at low nitrogen pressures (0.5 MPa), which is associated with a change in the energy characteristics of the activated powder.

The degree of ferrochrome nitriding tends to increase with increasing diameter of the sample because of a de-crease in the heat lost in the reactor volume. Over the pressure range examined, we did not observe combustion of samples less than 25 mm in diameter. The density of the samples in combustion affects substantially the nitrogen content in the combustion products. The nitrogen content in nitrided ferrochrome tends to increase with decreasing density. Therefore, to prepare ferrochrome with a high nitrogen content, we used free-flowing powder.

We examined the degree of ferrochrome nitriding in relation to the particle size and found that, under the actual conditions, there was no combustion of samples with the particle size over 80 μm, as well as up to 80 μm (40–63, 63–80 μm) though without a fine fraction.

Inspection of the burned samples showed that they comprise two prominent extensive zones: an internal, densely sintered compact zone, and an external, poorly sintered loose zone. The X-ray phase analysis showed that the composition of these zones depends on the nitrogen pressure. At nitrogen pressures above 6 MPa the main phase is chromium mononitride CrN both in the densely sintered segment and in the loose part of the sample. At 4–6 MPa the dominating phase in the sintered zone is mononitride, and the nonsintered part of the sample consists basically of Cr_2N. At pressures under 4 MPa the phase composition in both zones is represented primarily by Cr_2N. It should be noted that, with decreasing pressure, the densely sintered segment

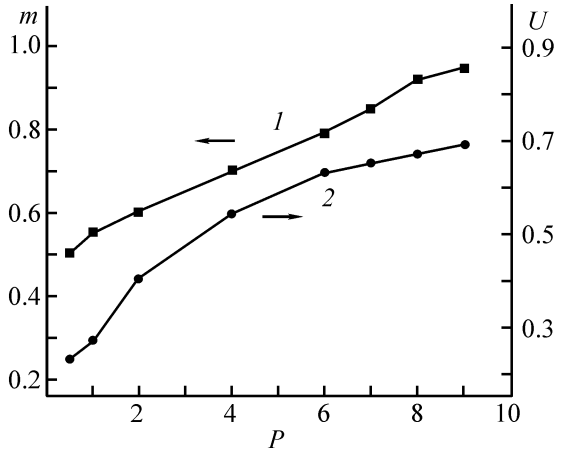

Fig. 2. (*1*) Degree of nitridation m and (*2*) combustion velocity u, mm s^{-1}, of ferrochrome vs. nitrogen pressure *P*, MPa.

considerably increases in size. For example, at the nitrogen pressure of 0.6 MPa this zone accounts for ca. 2/3 of the sample volume.

The heterogeneous macrostructure of the burned samples is most probably associated with the surface combustion mode in which the combustion velocity on the surface of the sample exceeds that in its interior. The burned surface layers are still gas-permeable, for which reason the filtration of nitrogen to the interior of the sample does not cease. When passing through the heated surface layer, nitrogen is heated, thereby increasing the temperature in the interior, which promotes sintering of the particles of the combustion products.

The sintered segment decreases in volume with increasing nitrogen pressure because the surface combustion mode becomes of less significance, which causes both the nitrogen filtration rate and concentration of the reacting gas in the sample pores to increase.

Thus, preparation of easily crushed nitrided ferrochrome cake with a high nitrogen content requires synthesis at nitrogen pressures above 8 MPa.

The X-ray phase analysis showed that the ferrochrome nitridation products contained α-iron, chromium mononitride CrN, chromium nitride Cr_2N, and complex nitride $(Cr, Fe)_2N$. With increasing nitrogen pressure in synthesis of nitrided ferrochrome the proportion of chromium mononitride tends to increase and that of complex nitride $(Cr, Fe)_2N$, to decrease, correspondingly (Fig. 3). Our experiments showed that a chromium mononitride–iron composition can be prepared at nitrogen pressure of 10 MPa and above.

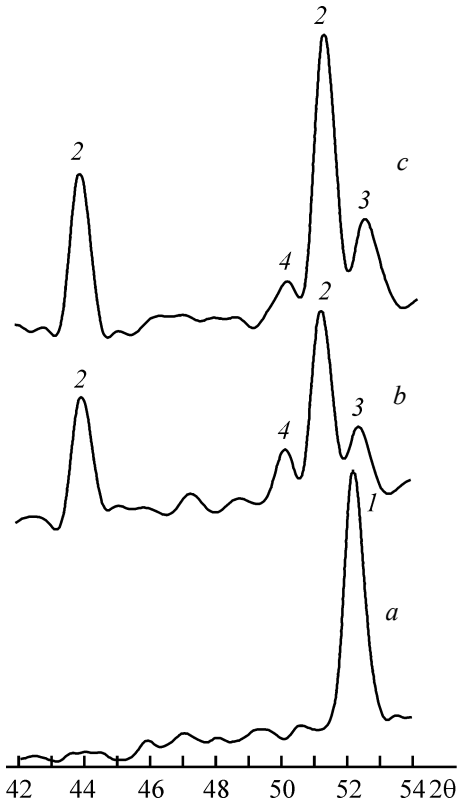

Fig. 3. Diffraction patterns of (a) initial and (b, c) nitrided ferrochrome at the nitrogen pressure of (b) 4 and (c) 7 MPa. (2θ) Bragg's angle. Composition of phases: (*1*) solid solution of Fe in Cr; (*2*) CrN; (*3*) Fe; and (*4*) $(Cr,Fe)_2N$. (*1*) *a*, (*2*) *b,* (*3*) *c*.

We examined acid enrichment of nitrided ferrochrome with the aim to isolate chromium mononitride both with polydisperse and fractionated powders. Chemical analysis of fractionated powders of nitrided ferrochrome showed that separation of the particles into fractions involved stratification of the nitride phases and iron. The fine powder was enriched in nitrides, and in the large-sized fraction the proportion of iron increased. For each fraction before acid enrichment we determined the content of iron. Figure 4 shows the time variation of the degree of acid enrichment for fractionated powders of nitrided ferrochrome. Meant by the degree of acid enrichment was the ratio of the amount of iron that passed into solution to that of iron contained in fractionated powder of nitrided ferrochrome before acid enrichment. As expected, the rate of passing of iron into solution tends to increase with decreasing particle size. The slowest process is the removal of iron from nitrided ferrochrome with the particle size of 80–160 μm.

We carried out electron-microscopic examination (Fig. 5) of the microstructure of the nitrided ferrochrome

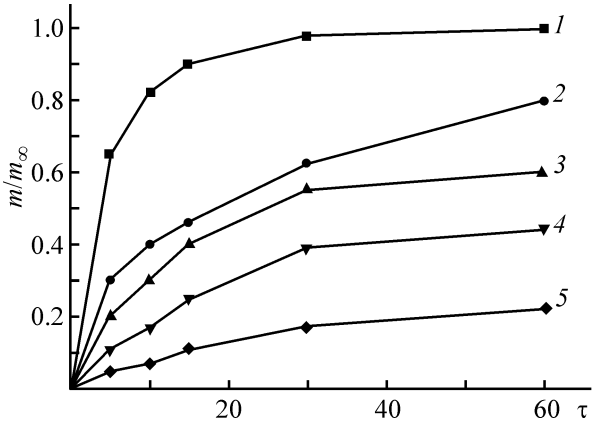

Fig. 4. Degree of acid enrichment of nitrided ferrochrome m/m_∞ vs. time of the process τ, min. Particle size, μm: (*1*) up to 5; (*2*) 10–15; (*3*) 15–40; (*4*) up to 40; and (*5*) 80–160.

fraction of interest and found that a part of iron occurs in closed (shown with arrows), and hence hardly accessible for the acid, sites of the composite alloy. The degree of acid enrichment and the run of the curves (Fig. 4, curves *3–5*) suggest that either exhaustive removal of iron in this case is impossible or the process takes very much time. The finer the powder, the higher the rate of passing of iron into solution, since during crushing individual particles of soluble iron-containing inclusions lose contact with the inert nitride matrix and are rapidly dissolved by the external diffusion mechanism. Thus, powder grain size is the factor deciding the rate of passing of iron into solution. For nitrided ferrochrome with a particle size under 5 μm virtually100% iron is removed within no longer than 0.5 h (Fig. 4, curve *1*).

We employed acid enrichment of the combustion products for preparing chromium nitride powder with the residual iron content of 0.3 wt%.

A raster electron-microscopic examination revealed some specific features of the microstructure of chromium nitride. The electron image (Fig. 6) clearly demonstrates the crystal growth steps. These steps are evidently associated with the dislocation mechanism of the crystals growth [8]. The growing crystals can differently respond to the presence of impurities in the crystallization medium, specifically, they either capture or reject the impurities. Probably, in this case, during the growth of the chromium nitride crystal, iron is rejected and accumulated near certain faces, thereby decelerating their growth, which is manifested in formation of a step.

It should be noted that the microstructure of chromium

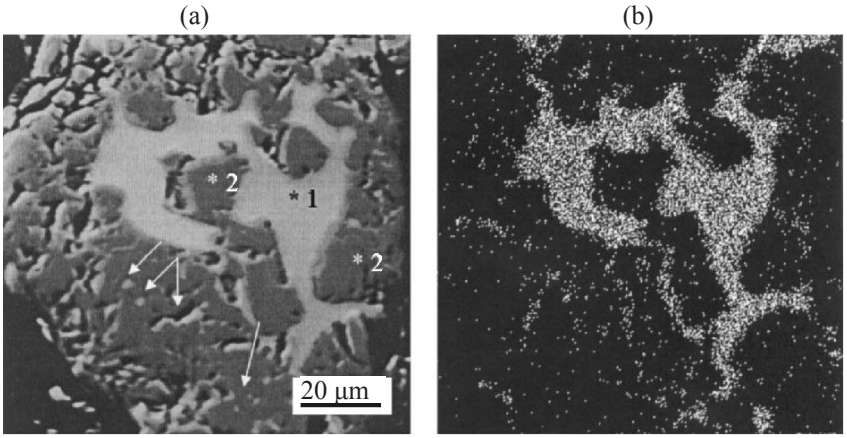

Fig. 5. Microstructure of nitrided ferrochrome: (a) in electron beams and (b) in FeKDα characteristic iron X-rays: (*1*) Fe and (*2*) CrN.

nitride prepared by the reaction of chromium with nitrogen in the combustion mode [9] does not exhibit characteristic growth steps, which can suggest the influence of iron on the crystal growth. The growth steps in chromium nitride can serve as sites of increased catalytic activity when chromium nitride is used as catalyst.

Study of the corrosion resistance of CrN in air showed that chromium nitride reacts with oxygen at temperatures within 910–1300°C, which agrees well with the data for CrN, obtained by other methods [10]. The maximum of the DTA peak was observed at 1084°C, and the heat effect of oxidation of chromium nitride was estimated at 450 ± 40 kJ mol^{-1}.

Levinskii et al. [11] found that chromium nitride has a low thermal stability and at atmospheric pressure dissociates at 1050°C. To determine the thermal stability of the resulting chromium nitride, the powder was heated in a helium atmosphere to 1430°C. The TG curve exhibited a mass loss of 0.5–2.0% at temperatures ranging from room temperature to 500–600°C. This is evidently due to removal of moisture and gases during storage via adsorption. Chromium mononitride is stable in a helium atmosphere up to 1015°C (mass loss of 0.6%), which is followed by two-stage decomposition. In the first stage, at temperatures within 1015–1246°C, chromium nitride is decomposed into Cr_2N and gaseous nitrogen, which results in a 10.4% mass loss with appreciable heat absorption (130 ± 12 kJ mol^{-1}). The DTA peak maximum corresponds to 1095°C. The second stage is observed at 1246–1430°C without appreciable heat effect in the DTA curve and with mass loss by another 5.7%. An X-ray phase examination showed that the products of decomposition at 1430°C contained chromium and chromium nitride (Cr_2N).

The decomposition onset temperature for the chromium nitride prepared in our experiments (1015°C) is lower than the published value (1050°C). This can be associated with increased defectiveness of the powder surface because of the action of acid.

Based on our findings, as well as on the data reported by Levinskii et al. [11], namely, that the dissociation temperature for chromium nitrides appreciably decreases with decreasing pressure, we heated chromium mononitride in a vacuum. This caused decomposition of chromium nitride by the reaction

$$2CrN \rightarrow Cr + N_2$$

Our experiments showed that the nitrogen concentration appreciably decreases at temperatures above 900°C, but vigorous gas evolution was observed at 1150–1250°C only. Keeping in a vacuum furnace at 1250°C for 3 h yielded

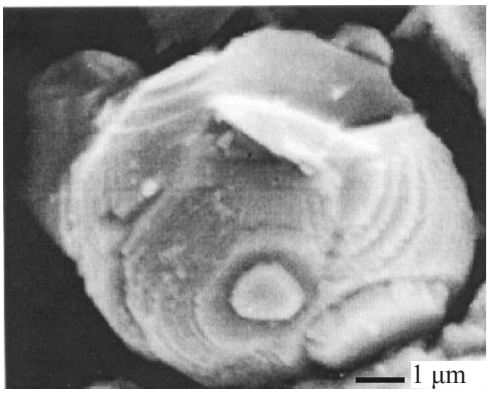

Fig. 6. Microstructure of chromium nitride prepared by acid enrichment of nitrided ferrochrome.

99.5% pure chromium metal, which is characteristic for some brands of electrolytic chromium.

CONCLUSIONS

(1) Chromium nitride can, in principle, be synthesized in a chromium nitride combustion wave with ferrochrome as reactant.

(2) The revealed relationships in combustion of ferrochrome in nitrogen suggest that the most significant synthesis parameters for chromium nitride in the combustion mode are the particle size distribution of the initial powder and nitrogen pressure. At pressures within 0.5–10 MPa the maximal degree of nitridation is reached under following conditions: pressure 10 MPa; bulk density of the sample; particles smaller than 80 μm (with <15 μm fraction dominating); samples over 30 mm in diameter.

(3) The acid enrichment rate is determined by the composition of the SHS–nitridation product and reaches a maximum for <5 μm fraction.

(4) A specific feature of the microstructure of the resulting chromium nitride consists in characteristic growth steps associated with the dislocation growth mechanism of the crystals and rejection of iron during CrN growth and its accumulation near certain faces. Further treatment with acid exposes the growth steps in chromium nitride, which can serve as sites possessing increased catalytic activity.

(5) Acid enrichment and subsequent vacuum heating of SHS-nitrided ferrochrome yielded 99.5% pure chromium.

This study was financially supported by the Russian Foundation for Basic Research, project no. 09-03-00604-a.

REFERENCES

1. Braverman, B.Sh., Ziatdinov, M.Kh., and Maximov, Yu. M., *Prepr. 2nd Int. Conf. on High-Nitrogen Steels*, Aachen (Germany), October 1990, Düsseldorf: Stahleisen mbh, 1990, p. 361.
2. Braverman, B.S., Ziatdinov, M.Kh., and Maksimov, Yu.M., *Fiz. Goreniya Vzryva*, 1999, vol. 35, no. 5, pp. 40–45.
3. RF Patent 2075870.
4. Shkoda, O.A., Terekhova, O.G., and Chalykh, L.D., *Samorasprostranyayushchiisya vysokotemperaturnyi sintez: Materialy i tekhnologii: sbornik nauchnykh trudov* (Self-Propagating High-Temperature Synthesis: Materials and Technologies: Coll. of Scientific Works), Novosibirsk, 2001, p. 216.
5. Korchagin, M.A., Grigor'eva, T.F., Bokhonov, B.B., et al., *Fiz. Goreniya Vzryva*, 2003, vol. 39, no. 1, pp. 51–59.
6. Rabinovich, A.V., Umarov, K., Sulaev, I.E., et al., *Izv. Vyssh. Uchebn. Zaved., Ser. Chern. Metal.*, 1975, no. 12, pp. 54–58.
7. Trusov, B.G., *Modelirovanie khimicheskikh i fazovykh ravnovesii pri vysokikh temperaturakh. ASTRA-4: Instruktisya dlya pol'zovatelei* (Modeling of Chemical and Phase Equilibria at High Temperatures. ASTRA- 4: User's Guide), Moscow: Mosk. Gos. Tech. Univ. im. N. E. Baumana, 1991, p. 35.
8. Egorov-Tismenko, Yu.K., Litvinskaya, G.P., and Zagal'skaya, Yu.G., *Kristallografiya* (Crystallography), Moscow: Mosk. Gos. Univ., 1992.
9. Bravermann, B.Sh., Lepakova, O.K., and Maksimov, Yu.M., Izv. *Vyssh. Uchebn. Zaved., Ser. Tsvet. Metal.,* 2008, no. 2, pp. 59–62.
10. Lyutaya, M.D., Kulik, O.P., and Kachkovskaya, E.T., *Poroshk. Metal*., 1970, no. 3, pp. 72–75.
11. Levinskii, Yu.V., *p–T–x-Diagrammy sostoyaniya dvoinykh metallicheskikh sistem* (p–T–x Phase Diagrams of Binary Metal Systems), Moscow: Metallurgiya, 1990.